



10th International Conference on Applied Energy (ICAE2018), 22-25 August 2018, Hong Kong, China

CO₂ gasification and pyrolysis reactivity evaluation of oil shale

Luyao Tang^{a,b}, Yuxin Yan^a, Yang Meng^{a,b}, Jiayu Wang^a, Peng Jiang^{a,b}, Cheng Heng Pang^a, Tao Wu^{a,b*}

^aDepartment of Chemical and Environmental Engineering, The university of Nottingham Ningbo China, Ningbo 315100, PR China

^bNew Material Institute, The University of Nottingham Ningbo China, Ningbo 315100, PR China

Abstract

This research focuses on the non-isothermal CO₂ gasification and pyrolysis reactivity via thermogravimetric analysis. It was found that CO₂ decreased activation energy of all four types of oil shale (Fushun, Jinzhou, Wulin, Xingsheng). Activation energy of XS oil shale was highly reduced from 59.86 kJ/mol to 9.48 kJ/mol. Reactivity index results showed that WL and XS oil shales were observed to be more dependent on CO₂ atmosphere. Alkali metal oxide also contributed to thermal decomposition according to thermogravimetric (TG) and differential thermal analysis (DTG) curves during CO₂ gasification process. Overall, CO₂ atmosphere can be used to improve oil shale decomposition, especially for alkali-rich shales, while providing an efficient and effective means to convert greenhouse gases into useful fuels.

© 2019 The Authors. Published by Elsevier Ltd.

This is an open access article under the CC BY-NC-ND license (<http://creativecommons.org/licenses/by-nc-nd/4.0/>)

Peer-review under responsibility of the scientific committee of ICAE2018 – The 10th International Conference on Applied Energy.

Keywords: oil shale; CO₂ gasification; pyrolysis

1. Introduction

Oil shale is an impermeable, combustible, naturally fine-grained brown material. A variety of complex heavy organic compounds, known as kerogen, are evenly distributed in mineral matrix (1). Oil shale reserves in China are estimated as nearly 4 billion tons, and due to its H/C atomic ratio, those reserves are considered as ideal alternative energy source (2, 3). However, low volatile content leads to low heating value of gas product, while particle size

* Corresponding author. Tel.: +86 156 0660 3288.

E-mail address: tao.wu@nottingham.edu.cn

requirement on feedstock restricts capacity, profit and efficiency as well as increases the complexity of oil shale plant. In order to enhance the product yield, multiple approaches such as flash pyrolysis, multi-stage pyrolysis and microwave-enhanced pyrolysis are used for oil shale thermal degradation process. All those techniques focus on getting higher efficiency, achieving diversified products and reuse residues at maximum level (4-6).

Conventional pyrolysis technology using pure nitrogen as carrier gas was conducted by numerous researchers (2, 7). Great achievements have been reached to show the effect of different heating parameters on pyrolytic products. However, utilization of CO₂ in oil shale gasification has caught rising attention in last few years due to the potential capability on CO₂ emission mitigation (8). Many benefits were investigated by previous researchers and showed positive impact on tuning H₂/CO ratio in syngas for various downstream industry (9).

Thermogravimetric analysis (TGA) is widely used for oil shale thermal decomposition kinetics. Many studies have concluded that weight loss during pyrolysis was combination of oil, water, gases and mineral decomposition (10, 11). However, TGA still provides a quantitative approach for detailed observations of pyrolysis behavior because of its high-accuracy assessment of many types of substances like oil shale, biomass and other blended mixtures (12). In this paper, the CO₂ gasification and pyrolysis reactivity of four different oil shale was measured by TGA. The alkali index, shale oil and syngas content, proximate and ultimate analysis and crystalline structure of each oil shale were correlated with gasification and pyrolysis reactivity. Moreover, the kinetic study was also used to compare the reactivity of four types of oil shale. Finally, the product quantity and quality changes were analyzed with respect to the impacts of reaction atmosphere as well as interactions between inherent minerals and organic matters.

2. Experimental sections

2.1. Sample preparation

Oil shale samples used in this work were obtained from four different mines in China: Fushun (FS) mine in Liaoning Province, Jinzhou (JZ) mine in Liaoning province, Xingsheng (XS) Mine in Heilongjiang province and Wulin (WL) mine in Heilongjiang province. Each type of lump oil shale was ground by jaw crusher (MSK-SFM-ALO) to less than 1500 μ m. Ground oil shale was sieved then 1 size range (1000-710 μ m) was selected for pyrolysis test and kinetic analysis and dried at 105 $^{\circ}$ C to constant weight then stored in a desiccator for use.

2.2. Measurement

Proximate analysis was conducted by thermogravimetric analyzer (TG-DSC, NETZSCH STA449F3, Germany). Proximate analysis shows different composition of moisture (M), volatile matters (VM), fixed carbon (FC) and ash (A) in oil shale samples. Carbon (C), hydrogen (H), Sulphur (S) and nitrogen (N) of oil shale were analyzed by CHNS/O Elemental analyzer (Euro Vector EA3000, Italy), and results are showed in Table 1.

Scanning Electron Microscope (SEM, Sigma VP, Zeiss) coupled with an Energy Dispersive X-ray Spectrometer (EDX, Oxford, UK) was used to achieve mineral composition of oil shale. 20 analysis sections were chosen for each type of oil shale to obtain average mineral composition value.

Table 1. Proximate and ultimate analysis of four types of oil shale.

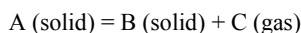
Properties	FS OS	JZ OS	XS OS	WL OS
Proximate analysis (wt%, raw basis)				
Moisture	1.33	0.81	1.12	6.88
Volatile	18.79	19.70	14.30	30.30
Fixed carbon	1.22	1.77	15.29	20.19
Ash	78.66	77.72	69.29	42.63
Ultimate analysis (wt%, dry ash free basis)				
C	47.23	50.46	63.03	38.04

H	6.06	7.68	4.33	2.88
N	6.80	6.01	1.88	1.54
O	35.95	30.60	29.54	56.58
S	3.97	5.24	1.23	0.95
H/C atomic ratio	1.54	1.83	0.82	0.91
HHV (MJ/kg)	4.12	4.70	7.87	15.03

3. Results

3.1. Kinetic analysis

In solid fuel non-isothermal kinetic analysis, the basic reaction was represented in the following (13):



The rate of kinetic process is normally put in the form:

$$\frac{dx}{dt} = k_0 f(x) \quad (1)$$

Where x is the extent of conversion, K_0 is the rate of constant and t was the time

$$x = \frac{\omega_0 - \omega}{\omega_0 - \omega_f} \quad (2)$$

The extent of conversion could be written as above. ω_0 and ω_f refer to values of initial weight and final weight. Based on Arrhenius law, the temperature related to the rate constant is defined in the following equation:

$$K_0 = A \exp\left(-\frac{E}{RT}\right) \quad (3)$$

E represents the activation energy and A is the pre-exponential factor. R is the gas constant, which is $8.314 \text{ J mol}^{-1} \text{ K}^{-1}$. Eliminating this equation with last equation

$$\frac{dx}{dt} = A \exp\left(-\frac{E}{RT}\right) f(x) \quad (4)$$

For non-isothermal conditions, β is used to represent constant heating rate $\beta = dT/dt$. The first order kinetics is assumed and substituting β into previous equations, where dt is replaced by β and dT .

The integral method was widely used for kinetic analysis of non-isothermal data. The method used in this work was based on following kinetic equation

$$\frac{dx}{dT} = \frac{A}{\beta} \exp\left(-\frac{E}{RT}\right) (1-x) \quad (5)$$

Therefore, taking natural log on the both sides produced the logarithmic form as following:

$$\ln\left(-\frac{\ln(1-x)}{T^2}\right) = -\frac{E}{RT} + \ln \frac{AR}{\beta E} \quad (6)$$

Plotting $\ln\left(-\frac{\ln(1-x)}{T^2}\right)$ against $1/T$ gives a fitting line having a slope of $-E/R$ and an intercept of $\ln AR/\beta E$. Activation energy E and pre-exponential factor A are derived from these values.

The activation of oil shale sample was determined by plotting linear form of the above logarithmic equation. Conversion extent in the range of 0.2-0.5 and 0.5-0.7 were selected for activation energy calculation, which was based on the weight loss curves. All R^2 values of linear fitting lines are above 0.90 thus suggesting high reliability. The activation energy is listed in table 2

Table 2. Activation energy of four oil shale under N₂/CO₂ atmosphere.

0.2-0.5	FS		JZ		WL		XS	
	E _a	R ²	E _a	R ²	E _a	R ²	E _a	R ²
N ₂	115.415	0.9987	148.962	0.9986	13.6358	0.9405	59.855	0.9928
CO ₂	96.027	0.9964	125.35	0.996	9.332	0.9248	9.48	0.944
0.5-0.7	FS		JZ		WL		XS	
	E _a	R ²	E _a	R ²	E _a	R ²	E _a	R ²
N ₂	77.92	0.9979	85.850	0.9893	26.496	0.9995	39.487	0.9995
CO ₂	47.908	0.9971	65.359	0.9784	3.817	0.9328	2.63	0.9288

Apparent from the table, good correlation was obtained for both conventional pyrolysis and CO₂ gasification process (R²>0.9). Among all four types of oil shale, FS and JZ oil shale samples showed relatively higher activation energy (>100kJ/mol) while WL and XS oil shale showed lower activation energy. This is possibly due to the different crystalline structure and mineral-organic interactions in different samples. That being said, a further reduction of 10-30kJ/mol in activation energy of all samples tested was observed when using CO₂ as processing atmosphere as long-chain organics are more likely to react and break into light hydrocarbons.

Reaction rate *r* can be determined by extent of conversion *x* and reaction time *t*

$$r = \frac{dX}{dt} \quad (7)$$

The average initial reactivity (R_i), the reactivity index (R_s) and the average final reactivity (R_f) were calculated following equation 8-10.

$$R_i = \frac{\sum_{X=0}^{X=0.1} r}{N} \quad (8)$$

$$R_s = \frac{0.5}{\tau 50} \quad (9)$$

$$R_f = \frac{\sum_{X=0.7}^{X=0.9} r}{N} \quad (10)$$

Where X, τ50 and N denotes the extent of conversion, the time needed for the conversion to reach 50% and number of data points, respectively.

According to reactivity results, FS and JZ oil shale have shown little changes throughout the entire process due to the high ash content as determined by proximate analysis in Table 1. The reactivity of WL and XS oil shale increased significantly during the initial and final stages, which can be attributed to the endothermic nature of CO₂-C reaction that has also been reported in other literature (13). Specific inherent minerals, such as carbonates, are difficult to decompose under CO₂ atmosphere, which resulted in slight reactivity change. Table 3 shows mineral composition (organic free basis) found in four types of oil shales. According to the mineral composition and ash content, it is obvious that ash content has remarkable influence on pyrolysis and CO₂ gasification reactivity. Higher ash content resulted in relatively lower reactivity, especially during the initial and final stages. However, an increase in alkali metal oxide composition, such as potassium oxide and calcium oxide led to higher reactivity This suggests that ash quality and quantity have profound impact of the thermal behavior of samples.

Table 3. Mineral composition in oil shale.

	FS	JZ	WL	XS
MgO	1.4%	1.4%	0.9%	0.9%
Al₂O₃	23.4%	25.7%	28.1%	26.4%
SiO	52.8%	56.9%	55.4%	61.5%

S	1.2%	0.7%	0.8%	0
K₂O	2.4%	1.9%	7.0%	4.9%
CaO	1.1%	2.2%	4.5%	3.5%
TiO₂	2.3%	1.6%	1.0%	1.9%
Fe₂O₃	15.4%	9.6%	2.3%	0.9%

Fig 1 and 2 show the non-isothermal decomposition profiles of oil shale samples which were pyrolyzed and/or CO₂-enhanced processed under same conditions. In both cases, oil shale experienced maximum weight loss within 300-600 °C. All four types of oil shale exhibited earlier decomposition in CO₂ gasification compared with pyrolysis test. WL and XS oil shale presented rapid decrease when temperature reached 150 °C. The maximum peak temperature of the WL and XS oil shale CO₂ gasification was lower by 5% and 30% than that of pyrolysis. However,

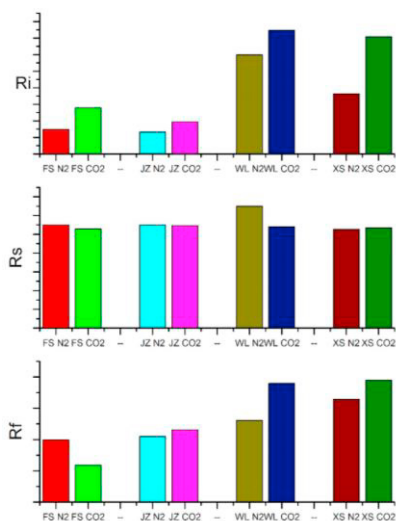


Fig.1. Reactivity index of four types of oil shale

no apparent trends were observed for FS and JZ samples which suggests that these samples are not responsive to CO₂ environment during gasification. This is possibly due to the high silica and aluminum oxide ratio and high ash content, which counteract the positive influences of alkali metals and CO₂ atmosphere.

4. Conclusion

The performance of CO₂ gasification and pyrolysis of four types of oil shales were compared in this work. It was found that WL and XS oil shales processing were improved by using CO₂ atmosphere. Kinetic analysis showed that activation energy was decreased for all four types of oil shales within conversion range of both 0.2-0.5 and 0.5-0.7. The more reactive nature of oil shale was linked to the lower percentage of ash and relatively higher content of alkali metal oxides. Comparison between non-isothermal CO₂ gasification and pyrolysis revealed the interactions between minerals, organic contents and reaction atmosphere resulted in positive synergistic effects, which iterates further CO₂ utilization possibilities in oil shale industry.

Acknowledgements

This work was partly supported by the Natural Science Foundation China (NSFC) [Grant Number 51650110508]. The International Doctoral Innovation Centre is also acknowledged for the provision of a full scholarship to the first and third authors.

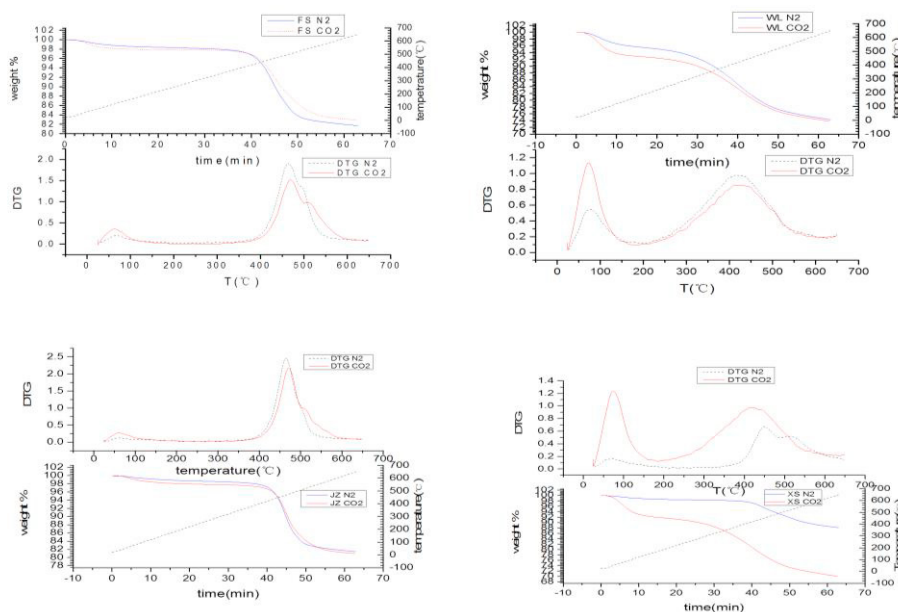


Fig.2. TG and DTG curves of four oil shale under N₂/CO₂ atmosphere

5. Reference

1. Yan J, Jiang X, Han X, Liu J. A TG–FTIR investigation to the catalytic effect of mineral matrix in oil shale on the pyrolysis and combustion of kerogen. *Fuel*. 2013;104(Supplement C):307-17.
2. Han H, Zhong N-n, Huang C-x, Zhang W. Pyrolysis kinetics of oil shale from northeast China: Implications from thermogravimetric and Rock–Eval experiments. *Fuel*. 2015;159(Supplement C):776-83.
3. Strizhakova YA, Usova T. Current trends in the pyrolysis of oil shale: A review. *Solid Fuel Chemistry*. 2008;42(4):197-201.
4. Wang S, Jiang X, Han X, Tong J. Investigation of Chinese oil shale resources comprehensive utilization performance. *Energy*. 2012;42(1):224-32.
5. Niu M, Wang S, Han X, Jiang X. Yield and characteristics of shale oil from the retorting of oil shale and fine oil-shale ash mixtures. *Applied Energy*. 2013;111(Supplement C):234-9.
6. Jiang X, Han X, Cui Z. New technology for the comprehensive utilization of Chinese oil shale resources. *Energy*. 2007;32(5):772-7.
7. Braun RL, Rothman AJ. Oil-shale pyrolysis: Kinetics and mechanism of oil production. *Fuel*. 1975;54(2):129-31.
8. Parvez AM, Wu T, Hong Y, Chen W, Lester EH, Mareta S, et al. Gasification reactivity and synergistic effect of conventional and microwave pyrolysis derived algae chars in CO₂ atmosphere. *Journal of the Energy Institute*. 2018.
9. Lahijani P, Zainal ZA, Mohammadi M, Mohamed AR. Conversion of the greenhouse gas CO₂ to the fuel gas CO via the Boudouard reaction: A review. *Renewable and Sustainable Energy Reviews*. 2015;41:615-32.
10. Bhargava S, Awaja F, Subasinghe ND. Characterisation of some Australian oil shale using thermal, X-ray and IR techniques. *Fuel*. 2005;84(6):707-15.
11. Burnham AK, Huss EB, Singleton MF. Pyrolysis kinetics for Green River oil shale from the saline zone. *Fuel*. 1983;62(10):1199-204.
12. Yao Z, Ma X, Wang Z, Chen L. Characteristics of co-combustion and kinetic study on hydrochar with oil shale: A thermogravimetric analysis. *Applied Thermal Engineering*. 2017;110(Supplement C):1420-7.
13. Wang Z, Deng S, Gu Q, Zhang Y, Cui X, Wang H. Pyrolysis kinetic study of Huadian oil shale, spent oil shale and their mixtures by thermogravimetric analysis. *Fuel processing technology*. 2013;110:103-8.
14. Ahmed II, Gupta AK. Kinetics of woodchips char gasification with steam and carbon dioxide. *Applied Energy*. 2011;88(5):1613-9.